

Insights into the nature of plasmon-driven catalytic reactions revealed by HV-TERS

Cite this: *Nanoscale*, 2013, 5, 3249

Zhenglong Zhang,^{ab} Li Chen,^a Mengtao Sun,^{*a} Panpan Ruan,^a Hairong Zheng^b and Hongxing Xu^{ac}

Received 10th November 2012

Accepted 22nd February 2013

DOI: 10.1039/c3nr00352c

www.rsc.org/nanoscale

The nature of plasmon-driven chemical reactions is experimentally investigated using high vacuum tip-enhanced Raman spectroscopy (HV-TERS). It is revealed that the coupling between the tip and the substrate can produce intense plasmon resonance, which then decays to produce sufficient hot electrons and thus catalyses the chemical reaction. The photoelectron emission from the laser illuminated silver substrate alone cannot drive the reaction.

Introduction

The *in situ* monitoring of plasmon-driven catalytic reactions is a rapidly growing area in the field of plasmon chemistry.^{1–10} Since the first experimental and theoretical reports of the plasmon-driven catalytic reaction of dimercaptoazobenzene (DMAB) produced from *para*-aminothiophenol,^{1,2} many investigations have been carried out to try and discover the mechanism of such reactions.^{1–10} Tip-enhanced Raman spectroscopy (TERS) in high vacuum is one of the best candidates for such investigations,^{11,12} since it can monitor and control the reaction processes *in situ* at specific catalytic sites with enormous surface sensitivity. Further, the use of the scanning probe microscopy (SPM) tip provides nano-scale spatial resolution, which is a significant improvement over the $\lambda_{ex}/2$ diffraction-limited spatial resolution in surface enhanced Raman scattering (SERS). In our previous work,⁹ we found that the density of the hot electrons generated from plasmon decay directly determines the rate and probability of a chemical reaction.⁹ However, to further reveal the mechanism in plasmon-driven catalytic reactions, a number of phenomena await further investigation, for example the

plasmonic thermal effect, the tip effect, the substrate effect, and identifying the source of the hot electrons in the reaction. Because HV-TERS can measure the Stokes and anti-Stokes Raman spectra *in situ* simultaneously,⁹ it is the perfect technique to study the plasmonic thermal effect.

In this communication, by utilizing the advantages of HV-TERS, we try to reveal the mechanism of the chemical reaction of 4-nitrobenzenethiol (4NBT) converting to DMAB. Firstly, since the tunneling current in the nanogap between the tip and substrate can be experimentally controlled and determines the size of the nanogap, thereby determining the plasmon intensity, we investigated the current dependence of the reaction rate. Secondly, we studied the contribution of the plasmonic thermal effect on the reaction by measuring and analyzing the Stokes and anti-Stokes TER spectra. We concluded that the catalytic effects in the reaction are primarily contributed by the hot electrons generated from plasmon decay rather than from the photoelectron emission of the tip or substrate.

Experimental and theoretical methods

Vibrational spectra were measured using a lab-built HV-TERS setup.⁹ It consists of a lab-built scanning tunneling microscope (STM) in a high vacuum chamber, a Raman spectrometer with a 632.8 nm He–Ne laser which incidents at 60° to the tip axis, and three-dimensional piezo stages for tip and sample manipulation. The objective was placed in the high vacuum chamber with a pressure of 10^{-7} Pa. A gold tip with a diameter of about 50 nm was made by the electrochemical etching of a 0.25 mm diameter gold wire.¹³ The substrates were prepared by evaporating 100 nm silver film onto newly cleaned mica films under high vacuum. The films were immersed in 1×10^{-5} M 4NBT in ethanol solution for 24 hours, then washed with ethanol for 10 minutes to ensure there was only one layer of molecules adsorbed on the silver film. Samples were put immediately into the high vacuum chamber. The TERS signals were excited with the 632.8 nm He–Ne laser.

^aBeijing National Laboratory for Condensed Matter Physics, Institute of Physics, Chinese Academy of Sciences, P. O. Box 603-146, Beijing, 100190, People's Republic of China. E-mail: mtsun@iphy.ac.cn

^bSchool of Physics & Information Technology, Shaanxi Normal University, Xi'an, 710062, People's Republic of China

^cSchool of Physics & Technology, Wuhan University, Wuhan, 430072, People's Republic of China

The wavelength-scanning plasmon enhanced spectroscopy of TERS was calculated using the finite difference time domain (FDTD) method,¹⁴ which is implemented in FDTD Solutions.¹⁵ The permittivity of Au and Ag was taken from the work of Palik.¹⁶

Results and discussion

The normal Raman spectra of 4NBT and DMAB produced from 4NBT can be seen in ref. 9 for reference. In the HV-TERS experiment, we simultaneously measured both the Stokes and anti-Stokes TER spectra of DMAB produced from the 4NBT molecules adsorbed on the Ag film with different tunneling currents, while the laser intensity and the bias voltage were kept fixed. Fig. 1(a) and (b) show the typical Stokes and anti-Stokes TER spectra of DMAB produced from 4NBT. They indicate that some of the 4NBT molecules have converted to DMAB. Moreover, six Raman peaks of DMAB can be clearly observed in the anti-Stokes TER spectrum. The experimental temperature can be fitted with eqn (1),

$$I_s/I_{as} = a e^{(\hbar\omega/k_B T)}, \quad (1)$$

where I_s and I_{as} are the intensities of the Stokes and anti-Stokes Raman, \hbar , k_B and T are the Plank constant, Boltzmann constant, and experimental temperature respectively, and a is an experimental constant. The current-dependence of the fitted experimental temperature and constant a are shown in Fig. 1(c) and (d). It can be seen that the experimental temperature does not depend on the current. However, our previous work showed that the Raman peak at 1336 cm^{-1} gradually decreases with the increase of current.⁹ These results indicate that, without a significant change in temperature, an increase in current leads to a decrease in the size of the nanogap between the tip and

substrate, and thus leads to an enhancement of the surface plasmon intensity and further promotes the chemical reaction.⁹ Therefore, the plasmonic thermal effect does not play an important role in the catalytic reactions. The reason might be that the thermal energy from the surface plasmon does not localize in the nanogap, but propagates very quickly and is dissipated along the tip or substrate. On the other hand, the fitted experimental constant a , as shown in Fig. 1(d), fluctuates between 2 and 3 with different currents.

As we know, the intensities of the Raman modes across the spectrum are strongly dependent on the plasmon wavelength. TER spectra can be most strongly enhanced when the excitation laser and the Raman scattering wavelengths are both efficiently coupled with the surface plasmon. Therefore, as the ratio of the intensities of the Stokes and anti-Stokes Raman spectra are used to estimate the experimental temperatures, in order to ensure the validation of the estimation, it is necessary to study both the Raman and plasmonic enhancement spectra. The tip-enhanced plasmonic excitation spectra were calculated at different sizes of the nanogap between the tip and substrate and are shown in Fig. 2(a) and (b). It was found that there is a strong plasmon resonance with a broad width around 632.8 nm in the tip-substrate system. Furthermore, the plasmon peak positions changed a little when the size of the nanogap was changed from 1 to 1.4 nm . The detailed analysis is discussed in Fig. 3 of ref. 17. Due to the symmetrical distribution of the plasmonic excitation spectra around 633 nm , our method to estimate the experimental temperatures using the Stokes and anti-Stokes TER spectra holds its validation for the 633 nm laser excitation wavelength.

To further support our claim that the plasmonic thermal effect does not play an important role in the catalytic reaction, we also studied the time- and laser intensity-dependent TER spectra. The collected time sequent TER spectra when the laser was set to 1% of its intensity are shown in Fig. 3(a). It can be observed that 4NBT did not undergo any chemical reaction at this laser intensity, indicating that the plasmon intensity is below the threshold of the chemical reaction. The laser intensity was increased to 10%, thus increasing the plasmon intensity, and the resulting time sequent TER spectra are shown in Fig. 3(b). This shows that new Raman peaks appear at 1387 and 1432 cm^{-1} , although the peak at 1336 cm^{-1} is still strong. These features indicate that a chemical reaction occurred and that 4NBT molecules were converted to DMAB. By computing the

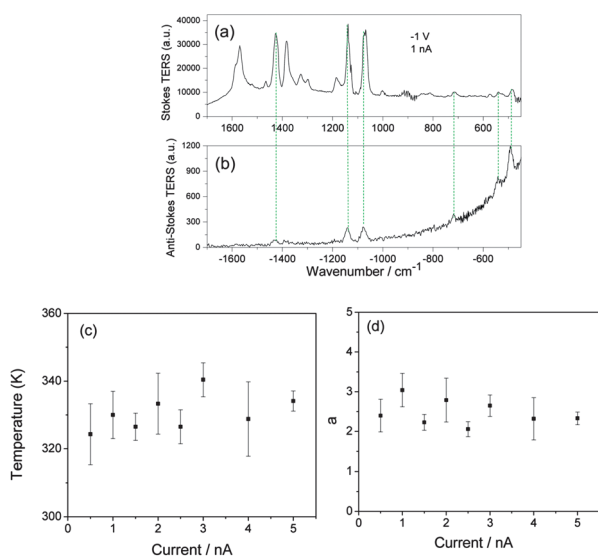


Fig. 1 (a) The Stokes and (b) anti-Stokes TERS of DMAB produced from 4NBT adsorbed on Ag film, (c) the current dependence of the experimental temperatures in the nanogap on TERS measurements, and (d) the fitted constant a from eqn (1).

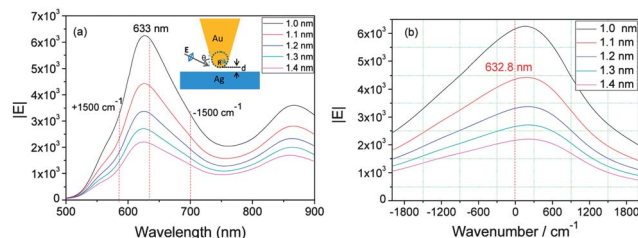


Fig. 2 The distance dependent wavelength-scanning plasmon enhanced spectrum of TERS, where R of the tip is 25 nm and $\theta = 60^\circ$.

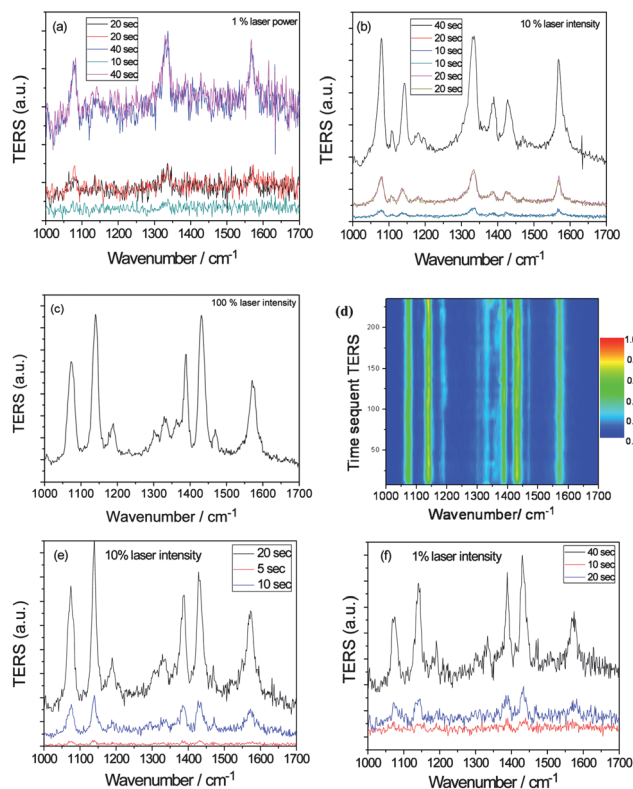


Fig. 3 The plasmon intensity controlled chemical reaction, where the plasmon intensity was controlled by the laser intensity at 1% (a), 10% (b), 100% (c and d), 10% (e) and 1% (f).

ratios between the intensities of the Raman peaks at 1432 cm^{-1} and 1568 cm^{-1} before (Fig. 1(a)) and after (Fig. 3(b)) the reaction, we can conclude that, at 10% laser intensity, the probability of a chemical reaction was below 40%. Further, from Fig. 3(b) it can also be seen that when the measurement time was increased, the probability of a chemical reaction did not change. The fact that an increase of measurement time did not yield a higher reaction probability could be explained because the thermal energy produced by the laser propagates and is dissipated quickly along tip and/or substrate. Therefore the thermal energy cannot be locally accumulated in the nanogap. When the laser intensity was further increased to 100%, the collected TER spectrum and time sequent 2D plot, shown in Fig. 3(c) and (d), revealed that the chemical reaction proceeded completely and reached a steady state. Next, when the laser intensity was decreased to 10% again, the observed TER spectra shown in Fig. 3(e) were the same as those in Fig. 3(c) and 1(a). Therefore, it can be concluded that the DMAB did not dissociate back to 4NBT again. To further confirm this, we decreased the laser power below the threshold again to its 1% intensity, and it can be seen that the resulting spectra in Fig. 3(f) were still the Raman spectra of DMAB.

With increasing laser intensity, hot electrons can be generated not only from plasmon decay, but also from photoelectron emission by the metal substrate and/or tip. It is, therefore, necessary to determine whether the photoelectrons injected from the metal can directly drive the chemical reaction. In the

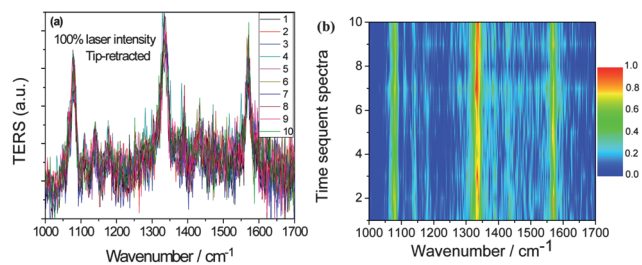


Fig. 4 (a) The time sequent TERS spectra, and (b) the 2D plot of time sequent tip-retracted spectra, where the tip is retracted for the measurement in HV-TERS. The numbers in the figure stand for the sequent measurements. The time interval between the measurement of spectra is 30 seconds.

experiment, we retracted the tip, chose another site on the substrate and measured tip-retracted spectra at 100% laser intensity. The time sequent tip-retracted spectra and 2D plot are shown in Fig. 4(a) and (b) respectively. It could be observed that the reaction did not occur without the tip, as in this case the intensity of the plasmon resonance on the substrate was too weak to produce enough hot electrons. Therefore, we can exclude the contribution of hot electrons produced from direct photoelectron injection from the substrate. The chemical reaction that converted 4NBT to DMAB must be driven by the hot electrons generated from plasmon decay.

From the above results, we concluded that in the tip-enhanced surface catalytic reaction, the tip significantly contributes to the plasmonic excitation intensity, which then decays and generates a high density of hot electrons and promotes the rate and probability of a reaction. Once DMAB is produced from 4NBT, it will not dissociate back to 4NBT with or without weak perturbation by 1% intensity laser illumination. To further support our conclusion, we measured successively the tip-retracted, tip-engaged and then the tip-retracted spectra again, all at the same spot with 100% laser intensity. The results are shown in Fig. 5(a)–(c) respectively. First, the tip-retracted

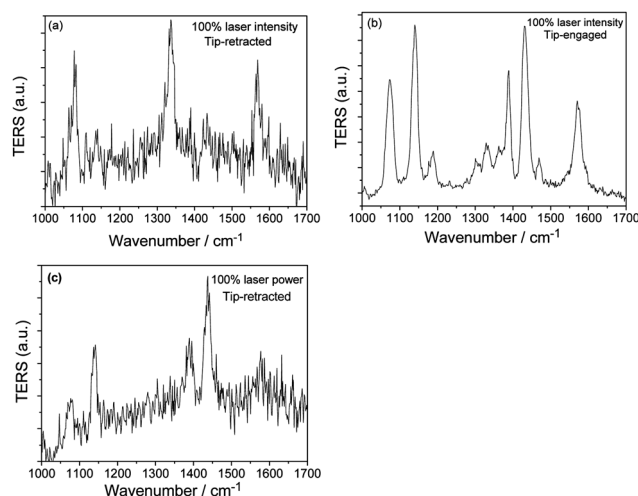


Fig. 5 The successively measured (a) tip-retracted, (b) tip-engaged and (c) tip-retracted spectra at same spot at 100% laser intensity.

spectrum shown in Fig. 5(a) revealed that, without the tip, the chemical reaction did not occur. Secondly, the tip-engaged spectrum, shown in Fig. 5(b), showed that some of the 4NBT was converted to DMAB, which was assisted by the strong plasmon intensity in the nanogap. Lastly, when the tip was retracted again, the spectrum shown in Fig. 5(c) is almost the same as that in Fig. 5(b), which indicates that the dimerized DMAB does not dissociate back to 4NBT again under weak plasmon intensity.

Conclusion and outlook

In summary, the mechanism of plasmon-driven catalytic reactions has been studied by performing Raman measurements with HV-TERS. It was found that the plasmonic thermal energy does not affect the chemical reaction equilibrium because the thermal energy from surface plasmon does not localize in the nanogap, but propagates and is dissipated quickly along the tip and substrate. Further, the calculated wavelength-scanning plasmonic excitation spectra revealed that the experimental temperatures estimated *via* the Stokes and anti-Stokes TER spectra are reliable. Moreover, the laser intensity-dependent Raman spectra and the tip-retracted spectra indicate that the hot electrons generated from plasmon decay drive the chemical reaction. Our experimental results demonstrate that surface catalytic reactions can be rationally controlled by many different parameters.

HV-TERS enables us to achieve atomic-resolution measurements and structural elucidation of adsorbed molecules on clean, single-crystal or nanostructured surfaces at low temperature. *In situ* spectral and topographical imaging can be conducted simultaneously, which provides an ideal technique to reveal the nature of chemical reactions. Further improvements include the use of femtosecond lasers for time-resolved TERS, which constitutes the most important part in the investigation of surface molecular reaction dynamics in our future experimental works.

Acknowledgements

This work was supported by the National Natural Science Foundation of China (Grants 90923003, 11274149 and

11174190), the National Basic Research Project of China (Grant 2009CB930701), the Fundamental Research Funds for the Central Universities (no. 2010ZYGX025), the Innovation Funds of Graduate Programs, SNU (no. 2010CXB004), and the Program of Shenyang Key Laboratory of Optoelectronic Materials and Technology (Grant no. F12-254-1-00).

Notes and references

- 1 Y. Fang, Y. Li, H. Xu and M. T. Sun, *Langmuir*, 2010, **26**, 7737.
- 2 Y. F. Huang, *et al.*, *J. Am. Chem. Soc.*, 2010, **132**, 9244.
- 3 H. Zhu, X. Ke, X. Yang, S. Sarina and H. Liu, *Angew. Chem., Int. Ed.*, 2010, **49**, 9657.
- 4 P. Christopher, H. Xin and S. Linic, *Nat. Chem.*, 2011, **3**, 467.
- 5 B. Dong, Y. R. Fang, X. W. Chen, H. X. Xu and M. T. Sun, *Langmuir*, 2011, **27**, 10677.
- 6 S. Gao, K. Ueno and H. Misawa, *Acc. Chem. Res.*, 2011, **44**, 251.
- 7 V. Joseph, C. Engelbrekt, J. Zhang, U. Gernert, J. Ulstrup and J. Kneipp, *Angew. Chem., Int. Ed.*, 2012, **51**, 7592.
- 8 Z. G. Dai, X. Xiao, Y. Zhang, F. Ren, W. Wu, S. Zhang, J. Zhou, F. Mei and C. Jiang, *Nanotechnology*, 2012, **24**, 335701.
- 9 M. T. Sun, Z. L. Zhang, H. R. Zheng and H. X. Xu, *Sci. Rep.*, 2012, **2**, 647.
- 10 M. van Schrojenstein Lantman, T. Deckert-Gaudig, A. J. G. Mank, V. Deckert and B. M. Weckhuysen, *Nat. Nanotechnol.*, 2012, **7**, 583.
- 11 H. Kim, K. M. Kosuda, R. P. Van Duyne and P. C. Stair, *Chem. Soc. Rev.*, 2010, **39**, 4820.
- 12 M. T. Sun and H. X. Xu, *Small*, 2012, **8**, 2777.
- 13 B. Ren, G. Picardi and B. Pettinger, *Rev. Sci. Instrum.*, 2004, **75**, 837.
- 14 K. S. Kunz and R. J. Luebber, *The Finite Difference Time Domain Method for Electromagnetics*, CRC Press, Cleveland, OH, 1993.
- 15 *FDTD Solutions, Version 7.5*, Lumerical Solutions, Inc., Vancouver, BC, Canada, 2011.
- 16 *Handbook of Optical Constants of Solids*, ed. E. D. Palik, Academic press, New York, 1985.
- 17 Z. Zhang, L. Chen, M. T. Sun and H. X. Xu, *Adv. Opt. Mater.*, submitted.